nature genetics

Bidirectional expression of CUG and CAG expansion transcripts and intranuclear polyglutamine inclusions in spinocerebellar ataxia type 8

Melinda L Moseley[1,2], Tao Zu[1,2], Yoshio Ikeda[1,2], Wangcai Gao[4], Anne K Mosemiller[1,2], Randy S Daughters[1,2], Gang Chen[4], Marcy R Weatherspoon[1,2], H Brent Clark[3,5], Timothy J Ebner[4], John W Day[2,5] & Laura P W Ranum[1,2]

We previously reported that a $(CTG)_n$ expansion causes spinocerebellar ataxia type 8 (SCA8), a slowly progressive ataxia with reduced penetrance. We now report a transgenic mouse model in which the full-length human SCA8 mutation is transcribed using its endogenous promoter. $(CTG)_{116}$ expansion, but not $(CTG)_{11}$ control lines, develop a progressive neurological phenotype with *in vivo* imaging showing reduced cerebellar-cortical inhibition. 1C2-positive intranuclear inclusions in cerebellar Purkinje and brainstem neurons in SCA8 expansion mice and human SCA8 autopsy tissue result from translation of a polyglutamine protein, encoded on a previously unidentified antiparallel transcript (ataxin 8, *ATXN8*) spanning the repeat in the CAG direction. The neurological phenotype in SCA8 BAC expansion but not BAC control lines demonstrates the pathogenicity of the $(CTG\text{-}CAG)_n$ expansion. Moreover, the expression of noncoding $(CUG)_n$ expansion transcripts (ataxin 8 opposite strand, *ATXN8OS*) and the discovery of intranuclear polyglutamine inclusions suggests SCA8 pathogenesis involves toxic gain-of-function mechanisms at both the protein and RNA levels.

Many dominant ataxias involve $(CAG)_n$ expansions translated into polyglutamine expansion proteins[1]. In contrast, the $(CTG)_n$ expansion mutation for spinocerebellar ataxia type 8 (SCA8) is transcribed, alternatively spliced and polyadenylated in the CTG orientation[2]. Because initial sequence analysis did not uncover any likely ORFs spanning the repeat in either direction, and because of the known pathogenic properties of CUG expansion transcripts in myotonic dystrophy, we proposed that SCA8 is caused by an RNA gain-of-function mechanism[2].

The SCA8 CTG expansion was isolated from a single individual with ataxia[3,4] and subsequently found in additional families with ataxia[4–9], including the seven-generation MN-A family (lod 6.8, $\theta = 0.0$)[4,10]. Affected individuals have gait and limb ataxia, dysarthria and nystagmus with mild spasticity in severely affected individuals[5,8–12]. Magnetic resonance imaging shows severe cerebellar atrophy without pontine or cerebral involvement[7,10] and pathological evaluation of human SCA8 shows Purkinje cell degeneration and loss of granule cells and inferior olivary neurons (unpublished observations, H.B.C., J.W.D. and L.P.W.R.).

The MN-A family shows a size-dependent penetrance, with affected members having larger expansions (mean = 119) than unaffected expansion carriers (mean = 90, $P = 5 \times 10^{-9}$)[10]. The reduced penetrance in the MN-A family is more pronounced in other SCA8 ataxia families regardless of repeat length[6,13–16]. This finding, and the discovery of SCA8 expansions in unaffected controls, has led to controversy and the suggestion that the SCA8 expansion is not pathogenic[6,13–18]. Our study of 37 SCA8 ataxia families supports a pathogenic role of the repeat and also suggests that other genetic or environmental factors affect penetrance[12]. To determine if the SCA8 expansion is pathogenic and to elucidate the molecular mechanisms of disease, we developed a transgenic mouse model in which the SCA8 mutation is present on a BAC. Two genes spanning the repeat are expressed in opposite directions: a newly discovered gene, ataxin 8 (*ATXN8*), which encodes a nearly pure polyglutamine expansion protein in the CAG direction, and ataxin 8 opposite strand (*ATXN8OS*, formerly *SCA8* or *KLHL1AS*), which, when transcribed, results in a noncoding CUG expansion RNA.

RESULTS

Generation and characterization of BAC transgenic mice

We developed SCA8 transgenic mouse models using the endogenous human promoter on a BAC clone to express the CTG with either a normal or expanded repeat tract (**Fig. 1a**). We selected BAC RP11-7o24 because the large amount of flanking sequence is likely to

[1]Department of Genetics, Cell Biology, and Development, [2]Institute of Human Genetics, [3]Department of Laboratory Medicine and Pathology, [4]Department of Neuroscience and [5]Department of Neurology, University of Minnesota, Minneapolis, Minnesota 55455, USA. Correspondence should be addressed to L.P.W.R. (ranum001@umn.edu).

Received 9 January; accepted 22 May; published online 25 June 2006; doi:10.1038/ng1827

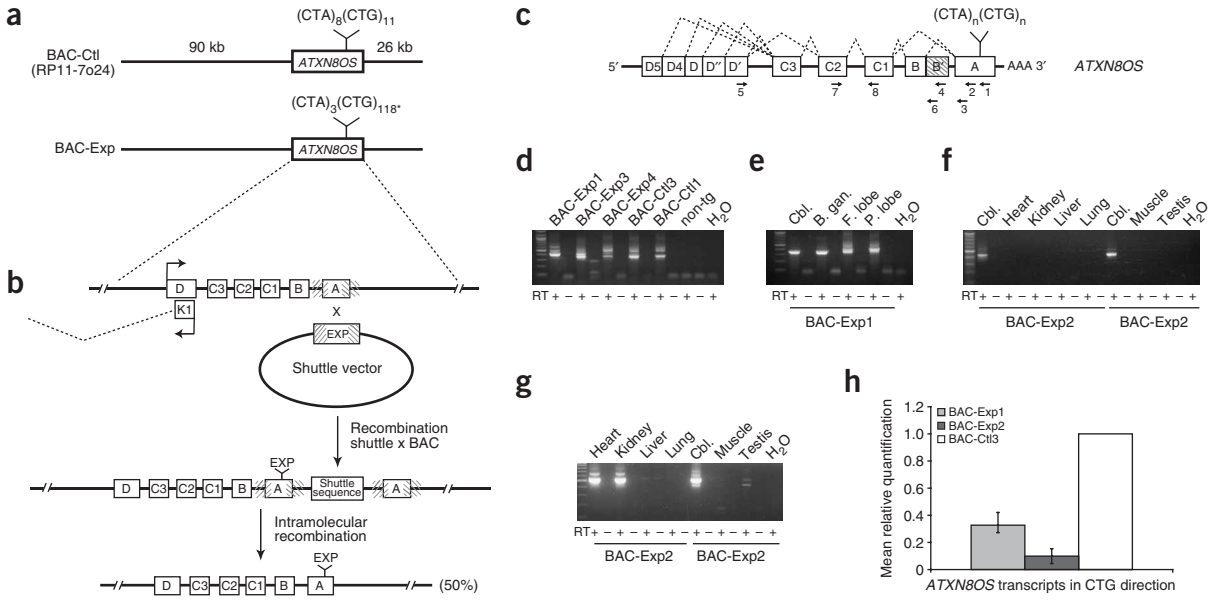

Figure 1 BAC expansion and control constructs. (**a**) Diagram of control BAC (BAC-Ctl) and modified BAC with SCA8 expansion (BAC-Exp) showing relative position of *ATXN8OS* and flanking sequence. * indicates the CTG repeat tract is interrupted with overall configuration of $((CTA)_3\ (CTG)_5CCG(CTG)_7\ CCG(CTG)_{104})$. (**b**) Homologous recombination strategy to incorporate SCA8 expansion into RP11-7o24 BAC. Cross-hatched boxes indicate ~500 bp of DNA flanking the repeat where recombination between the BAC and the shuttle vector takes place. Exons of the *ATXN8OS* gene (**a**–**d**) and the first exon of overlapping *KLHL1* gene (K1) are indicated by boxes; arrows show direction of transcription. (**c**) RT-PCR strategy with primers used for detection of *ATXN8OS* CUG transcripts. (**d**) Expression of transcripts containing *ATXN8OS* exon A in the cerebellum of high- (BAC-Exp1), medium- (BAC-Exp3) and low- (BAC-Exp4) copy expansion lines and two BAC control lines (BAC-Ctl1 and BAC-Ctl3). non-tg, nontransgenic. (**e**) Expression of transcripts containing *ATXN8OS* exon A in the BAC-Exp1 animal are shown: cerebellum (Cbl.), basal ganglia (B. gan.), frontal lobe (F. lobe) and parietal lobe (P. lobe). (**f**) RT-PCR results for splice forms containing exon A in non-CNS tissues from two BAC-Exp2 animals. (**g**) RT-PCR results for splice forms ending in exon B′. + and – represent presence or absence of reverse transcriptase. Ladder shows DNA size marker in 100-bp increments. (**h**) Histogram showing mean relative quantification (RQ) values of quantitative RT-PCR analysis to detect *ATXN8OS* transcripts in BAC-Exp1, BAC-Exp2 and BAC-Ctl3 lines. Error bars indicate s.e.m. of the dCt values for each group.

contain the regulatory elements required for accurate temporal and tissue-specific *ATXN8OS* expression[19]. With the exception of the first exon and part of the first intron of the overlapping *KLHL1* gene, no other known or predicted genes lie on this BAC. A pathogenic expansion and ~500 bp of sequence flanking the repeat from an affected MN-A family member was amplified by PCR, cloned into a shuttle vector and incorporated into the BAC by homologous recombination in *E. coli* (**Fig. 1b**)[19]. The recombinant BAC has an interrupted SCA8 expansion consisting of three CTAs and 116 interrupted CTGs $((CTA)_3(CTG)_5CCG(CTG)_7CCG(CTG)_{104})$, the same configuration in the affected MN-A individual.

We established seven lines containing expansions (BAC-Exp) and three control lines (BAC-Ctl). Three of the BAC-Exp lines and the three BAC-Ctl lines have a single copy of the BAC, and the remaining BAC-Exp lines have copy numbers of 2, 5, 9 and 13 (**Table 1**), as estimated by DNA blot. The CTG repeat size is fairly stable, with variations of one to five repeats detected by PCR (data not shown) in generations 1–5.

ATXN8OS expression in BAC transgenic lines

We used an RT-PCR strategy to detect *ATXN8OS* transcripts containing exon A (**Fig. 1c**) in both BAC-Exp and BAC-Ctl lines (**Fig. 1d**). We detected CUG-containing *ATXN8OS* transcripts by RT-PCR using exon A primers located 3′ or 5′ of the repeat tract for first-strand synthesis (primers 1 and 2, respectively). All ten transgenic BAC lines showed *ATXN8OS* expression of CUG-containing transcripts using nested primer sets 5 and 3; however, for the single-copy expansion lines, expression was variable, with transcripts detected in some but not all animals tested (data not shown). RT-PCR products containing exon A vary in size from 360–710 bp, depending upon alternative splicing; we sequenced them to confirm that they represented alternative splice forms of the *ATXN8OS* transcripts depicted in **Figure 1c**. Consistent with the low steady-state levels of *ATXN8OS* CUG transcripts in humans[4], *ATXN8OS* transcripts in the BAC-transgenic mice were detectable by RT-PCR but not RNA blot, with expression throughout the central nervous system (CNS), including in the cerebellum, basal ganglia, frontal lobe, parietal lobe (**Fig. 1e**) and spinal cord (data not shown). Non-CNS tissues were negative for expression of the exon A form containing the SCA8 repeat (**Fig. 1f**); however, an alternate *ATXN8OS* splice form ending in exon B′, which does not contain the CUG repeat, is expressed in heart, kidney, testis and CNS (**Fig. 1g**). We confirmed that these RT-PCR products contain Exon B′ by sequencing; products varied in size from 530–710 bp.

We determined relative expression of *ATXN8OS* transcripts in selected lines by quantitative RT-PCR. Expression was comparable between the BAC-Ctl3 mice and the BAC-Exp1 line, which has the highest copy number (13 copies). Expression in BAC-Ctl3 mice was significantly higher than in the BAC-Exp2 line, which has the second highest copy number (9 copies). Relative quantification value (RQ) = 0.33 for BAC-Exp1 versus BAC-Ctl3 (analysis of variance (ANOVA) $F_{2,6} = 6.228$, $P = 0.334$). RQ = 0.10 for BAC-Exp2 versus BAC-Ctl3 ($P = 0.029$) (**Fig. 1h**). In BAC-Exp5 animals, expression levels were too low for reliable quantification using a single round of RT-PCR.

Table 1 Summary of SCA8 BAC transgenic lines

BAC Line	Copy no.	CNS express. of CUG transcript	CNS express. of CAG transcript	1C2 Inclusions	Rotarod, 26 wks (P)	Penetrance 6–12 mos	Penetrance 12–18 mos	Penetrance 18–24 mos	On-beam (200 μA) $\Delta F/F$	Off-beam (200 μA) $\Delta F/F$	Off-beam (50 μA) $\Delta F/F$	Bic. resp. (on-beam) (%)	Bic. resp. (off-beam) (%)
Ctl1	1	Positive RQ = n.d.	n.d.	None detected	n.d.	No abnor obs	0/13	0/4					
Ctl2	1[a]	Positive RQ = n.d.	n.d.	None detected	n.d.	0/7	No abnor obs	0/3					
Ctl3	1	Positive level: RQ = 1	Positive level: RQ = 1	None detected	Not signif	No abnor obs	0/26	0/11	0.74 ± 0.02	–0.08 ± 0.05	–0.14 ± 0.02	26.1 ± 2.8[d]	–193.0 ± 63.5[d]
FVB	–	–	–	–	–	–	–	–	0.62 ± 0.12	–0.19 ± 0.16	–0.07 ± 0.06	47.3 ± 27.5[d]	–311.2 ± 183.0[d]
Exp1	13	Positive level: RQ = 0.33	Positive level: RQ = 2.1	Positive	9×10^{-6}	21/24[b] (**88%**)	Not quant	Not quant					
Exp2	9	Positive level: RQ = 0.10	Positive level: RQ = 0.06	Positive	3×10^{-4}	19/31[b] (**61%**)	Not quant	Not quant	1.21 ± 0.46[c]	0.14 ± 0.37[c]	0.05 ± 0.02[c]	1.24 ± 21.2	12.6 ± 24.7
Exp3	5	Positive RQ = n.d.	n.d.	n.d.	Not signif	2/7 (**29%**)	8/34 (**24%**)	11/21 (**52%**)					
Exp4	2	Positive RQ = n.d.	n.d.	n.d.	4×10^{-4}	0/24	6/38 (**16%**)	4/14 (**28%**)					
Exp5	1	Positive RQ = too low	Positive RQ = too low	None detected	Not signif	No abnor obs	7/12 (**58%**)	23/35 (**66%**)	0.93 ± 0.14	0.12 ± 0.07[c]	0.03 ± 0.02[c]	–0.04 ± 0.17	0.06 ± 0.06
Exp6	1	Positive RQ = n.d.	n.d.	n.d.	Not signif	No abnor obs	0/4	3/20 (**15%**)					
Exp7	1	Positive RQ = n.d.	n.d.	n.d.	Not signif	0/24	0/12	11/28 (**39%**)					

Exp = expansion line; Ctl = control line; no abnor obs: no abnormalities observed during routine cage observation and qualitative gait observation, but not quantitated; n.d. = not done; RQ = relative quantification by real-time RT-PCR normalized to BAC-Ctl3 line. On- and off-beam results are $\Delta F/F$ (mean ± s.d.); bicuculline response is percentage change in the $\Delta F/F$ (mean ± s.d.). The BAC-Exp2 line on-beam response was not significantly different from BAC-Exp5 line but was significantly greater than FVB or BAC-Ctl3 animals ($F = 3.93$ and post-hoc test, $P < 0.05$). The off-beam responses of both FVB and BAC-Ctl3 controls were not significantly different but were significantly different from the BAC-Exp2 and BAC-Exp5 lines for both 200 μA ($F = 9.10$ and post-hoc test, $P < 0.05$) and 50 μA stimulation ($F = 33.9$ and post-hoc test, $P < 0.05$). The $GABA_A$ antagonist bicuculline increased the on-beam response and reduced the off-beam response in both control lines ($P < 0.05$, paired Student's t-test) but had no significant effects in the BAC-Exp2 and BAC-Exp5 lines ($P > 0.05$). [a]Incomplete BAC. [b]Penetrance was evaluated based on cage behavior, except for the two highest–copy number lines, for which the number of animals that had died at 12 months is given. [c]Significant intensity difference among different animal lines (ANOVA followed by Duncan's test, $P < 0.05$). [d]Significant difference before and after bicuculline application in the same line (paired Student's t-test, $P < 0.5$).

BAC expansion mice have a progressive neurological phenotype

All seven BAC-Exp lines display a progressive neurological phenotype not present in BAC-Ctl lines. Expansion lines with the highest copy number, BAC-Exp1 and BAC-Exp2, develop a severe, fully penetrant phenotype (see **Supplementary Video 1** online, which shows a BAC-Exp2 animal at 20 weeks) in which animals become inactive, lose weight and die prematurely, with survival ranging from 4–18 months (**Fig. 2a** and **Table 1**). High-copy expansion lines show marked motor deficits at 16 weeks, including stiffness and posturing, with hind limbs fully extended and unable to relax (**Fig. 2b**), and generalized wasting, kyphosis and priapism at the end stage of the disease (**Fig. 2c**).

Animals from the five remaining BAC-Exp lines (one to five copies of BAC) generally develop milder, later-onset motor deficits, including abnormal gait, low stance and hind limb dragging between 6–18 months of age (**Fig. 2d**, **Table 1** and **Supplementary Video 2** online, showing a BAC-Exp5 animal at 19 months), but occasionally these animals develop more severe phenotypes that include wasting, stiffness and priapism similar to higher-copy BAC-Exp lines. As in human SCA8, low-copy BAC expansion lines have reduced disease penetrance (**Table 1**).

Consistent with the early-onset phenotype of the high-copy lines, animals from the BAC-Exp1 and BAC-Exp2 lines perform significantly worse on the rotarod at 26 weeks than both age-matched nontransgenic littermates and older (52 weeks) BAC-Ctl3 animals (**Table 1** and **Fig. 2e**). Although the BAC-Exp4 line shows a late-onset motor phenotype similar to other low-copy expansion lines at >1 year of age, the rotarod differences at 26 weeks probably reflect an additional hyperactivity phenotype only observed in this line caused by a separate insertion effect. We did not observe any similar motor phenotypes in any of BAC-Ctl lines through 2 years of age (**Table 1** and **Supplementary Video 3** online, showing a BAC-Ctl1 animal at 18 months).

Histological evaluation of BAC-transgenic lines

Histological analysis of the entire brain and spinal cord by hematoxylin and eosin (H&E), glial fibrillary acidic protein (GFAP) and Luxol fast-blue staining did not show any obvious neurodegenerative changes. We did not find either neuronal loss or gliosis in the motor cortex and the basal ganglia of the BAC expansion lines (BAC-Exp1, BAC-Exp2 and BAC-Exp5) compared with nontransgenic animals (data not shown). The cerebral hemispheric white matter and the corticospinal tracts through the spinal cord are also intact, without evidence of loss of myelinated fibers or primary demyelination. Examination of Purkinje cells by calbindin staining in these high- and low-copy BAC expansion lines did not uncover any apparent abnormalities (**Fig. 2f,g**). To determine if a direct effect on muscle or anterior horn cells could be involved, we performed histological and

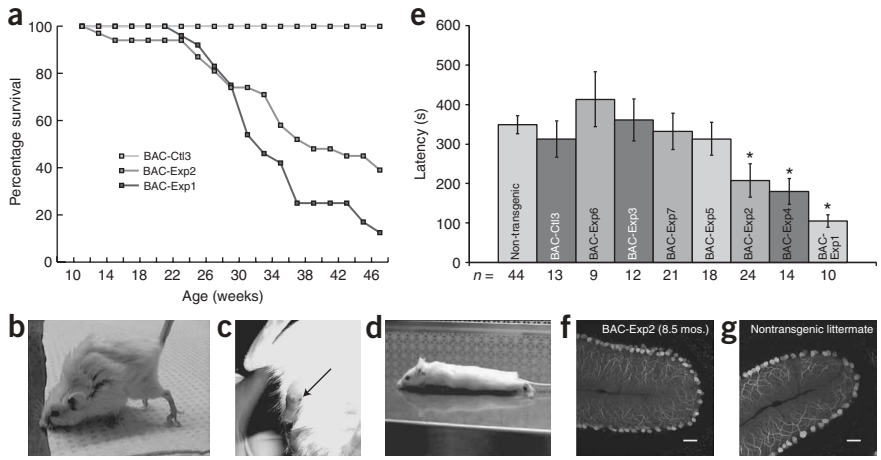

Figure 2 Progressive neurological phenotype in BAC expansion mice. (**a**) Survival curves for BAC-Exp1 and BAC-Exp2 animals compared with BAC-Ctl3 animals. (**b**) Severely affected mouse from BAC-Exp1 line showing kyphosis (curvature of the spine) and abnormal posturing. (**c**) Priapism (sustained penile erection) in severely affected male. (**d**) Animal from low-copy number line (BAC-Exp5) showing broad-based posture with low center of gravity. (**e**) Rotarod analysis of SCA8 BAC-Exp and nontransgenic animals at 26 weeks and BAC-Ctl3 animals at 52 weeks of age. Values shown are the amount of time animals were able to stay on the rotarod and are day 4 averages of all four trials. Statistically significant differences are indicated by asterisks. Error bars represent the standard error of the mean (S.E.M.). (**f**,**g**) Calbindin antibody staining shows grossly normal Purkinje cell morphology at 8.5 mos. in an affected BAC-Exp2 mouse (**f**) and its age-matched nontransgenic littermate (**g**). Scale bar = 50 μm.

electromyographic evaluation of skeletal muscle from BAC expansion lines but did not observe any pathological changes suggestive of denervation or myopathy or any functional changes such as myotonia (data not shown). We performed RNA FISH to look for CUG-containing ribonuclear inclusions in Purkinje cells or other cerebellar neurons but did not find CUG RNA foci (data not shown).

BAC-Exp mice have deficits in cerebellar inhibition

The progressive movement disorder in our BAC-Exp mice, the cerebellar effects of SCA8 in humans and the expression of CUG expansion transcripts in the cerebellum suggested that the phenotype in our mice could be caused by system-level changes in cerebellar function[20]. To test for functional deficits in the cerebellar cortex, we used *in vivo* optical imaging of flavoprotein autofluorescence to compare the effects of parallel fiber stimulation in the BAC-Exp mice (BAC-Exp2, $n = 4$, BAC-Exp5, $n = 4$) with nontransgenic (FVB, $n = 4$) and BAC control (BAC-Ctl3, $n = 3$) animals (**Fig. 3** and **Table 1**). These studies show that relative to nontransgenic FVB and BAC-Ctl lines, high- and low-copy BAC-Exp animals have a stronger on-beam excitatory response to parallel fiber stimulation ($P < 0.05$) and loss of the off-beam inhibitory response to both low and high-amplitude intensity stimulation ($P < 0.05$). Bicuculline increased the on-beam response and decreased the off-beam response in controls but had no effect in the BAC-Exp mice (**Fig. 3f** and **Table 1**). Taken together, these data demonstrate that the SCA8 CTG expansion alters the cerebellar cortical circuitry and that molecular-layer GABAergic inhibition is not functioning normally in both high-copy and low-copy BAC expansion lines.

1C2-inclusions in BAC-Exp mice and human SCA8 brains

To investigate molecular mechanisms that could explain the phenotypic features in our BAC-Exp mice, we reconsidered the possibility that the SCA8 expansion might be translated. Although sequence analysis did not predict likely ORFs, conceptual translation of a short downstream ORF spanning the repeat in the CTG direction would encode a polyleucine expansion protein and in the CAG direction a methionine immediately and only followed by a polyglutamine repeat tract (**Fig. 4a**). Because both polyleucine and polyglutamine containing expansion proteins have been reported to form intranuclear inclusions that are recognized by the 1C2 monoclonal antibody[1,21], we performed immunohistochemistry on our mice using the 1C2 antibody and antibody to ubiquitin (**Fig. 4**). Unexpectedly, 1C2-positive intranuclear inclusions were found in a subset of Purkinje cells and pontine neurons, including basal-pontine nuclei from both high-copy BAC expansion lines (BAC-Exp1 and BAC-Exp2; **Fig. 4b–d**) but not from low-copy BAC expansion animals (BAC-Exp5; data not shown), BAC control animals (BAC-Ctl3; **Fig. 4e–g**) or nontransgenic animals (**Fig. 4h–j**). We found similar 1C2-positive intranuclear inclusions and pan-nuclear staining in Purkinje, medullary and dentate neurons from human SCA8 autopsy tissue (**Fig. 4n–p**) but not from human control tissue (**Fig. 4q–s**). The 1C2-positive inclusions and pan-nuclear staining found in this SCA8 MN-A individual seem limited to the cerebellum and brainstem, with no evidence of inclusions or pan-nuclear staining elsewhere in the CNS, including cerebrum and spinal cord (data not shown). Although cerebellar slides were available from a second SCA8 individual, no Purkinje cells remained, preventing a similar analysis. In addition, inclusions

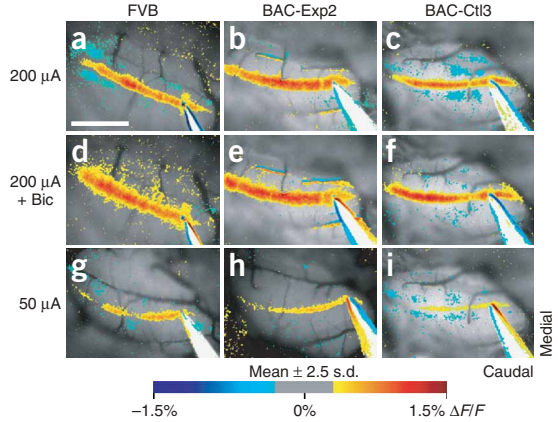

Figure 3 Responses to parallel fiber stimulation in FVB, BAC-Exp and BAC-Ctl mice. For each line of mice, the optical responses to 200 μA stimulation without (**a–c**) and with (+ Bic, **d–f**) 100 μM bicuculline and the responses to 50 μA stimulation (**g–i**) are shown. Statistically significant responses were pseudocolored (with increases shown in red and yellow and decreases in blue) and superimposed on a background fluorescence image of the folia. The gray region is the background fluorescence level used to define the significance threshold (mean ± 2.5 s.d.). Scale bar is 1 mm. For the FVB and BAC-Exp2 mice, the results using 50 μA stimulation are from different animals than the results obtained with 200 μA stimulation with and without bicuculline.

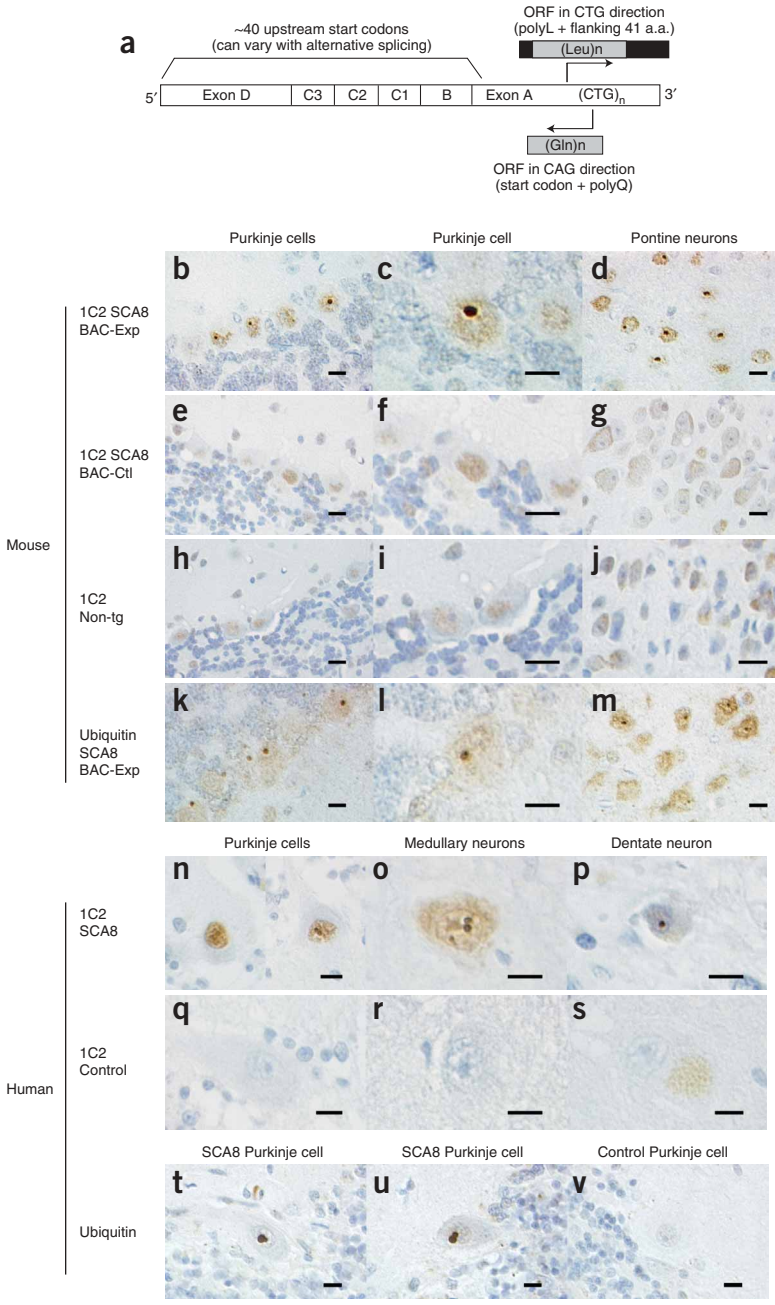

Figure 4 BAC-Exp animals and SCA8 autopsy brain have 1C2- and ubiquitin-positive intranuclear inclusions. (**a**) *ATXN8OS* Gene map. Conceptual translation shows that the short ORFs spanning the repeat encode a polyleucine expansion protein in the CTG direction and a methionine followed by a polyglutamine expansion in the CAG direction. In BAC-Exp mice, 1C2-positive intranuclear inclusions are evident in the Purkinje cells and pontine neurons (**b**–**d**), whereas no inclusions are seen either in BAC-Ctl (**e**–**g**) or nontransgenic (non-tg) littermates (**h**–**j**). In human SCA8 autopsy brain, 1C2-positive intranuclear inclusions and pan-nuclear staining are found in Purkinje, medullary and dentate neurons (**n**–**p**), whereas no inclusions are found in control brain (**q**–**s**). For both mice (**k**–**m**) and humans (**t**,**u**), inclusions are positive for ubiquitin, unlike staining in control animals (data not shown) or control human autopsy brain (**v**). Scale bars = 10 μm.

found in high-copy BAC expansion lines (BAC-Exp1 and BAC-Exp2) and this SCA8 patient are ubiquitin-positive (**Fig. 4k–m,t,u**), with no ubiquitin-positive inclusions in BAC-Ctl (data not shown) or human control brain (**Fig. 4v**). Because the 1C2 antibody was generated against the polyglutamine encoding TATA binding protein (TBP)[22], we performed immunohistochemistry using an antibody to TBP to determine if the 1C2 inclusions result from an accumulation of TBP, but we found no evidence for TBP accumulation (**Supplementary Fig. 1** online).

1C2-protein (ataxin 8) translated from polyglutamine ORF

To determine if the SCA8 expansion can encode a 1C2-positive protein, we performed a series of cell culture and *in vitro* translation experiments. Transient transfection of HEK293 cells with the full-length cDNA (CMV-exons DCBA) or a truncated minigene (CMV-exon-A) containing the expansion (**Fig. 5a**) led to expression of a ~40-kDa 1C2-positive protein (**Fig. 5b**). Additionally, variation in size of the 1C2 protein with repeat length demonstrates that the protein is translated from codons spanning the repeat (**Fig. 5c**) and expression of the SCA8 expansion results in the formation of 1C2-positive aggregates (**Fig. 5d**).

To determine if the 1C2 protein contains a polyleucine expansion, we performed the following transfections: (i) an exon A construct in which the polyleucine ORF was tagged with myc and His; (ii) a construct designed to force expression of a tagged polyleucine expansion protein by cloning the polyleucine ORF immediately downstream of a Kozak consensus sequence and (iii) a construct identical to construct (ii), with the addition of a stop codon (**Fig. 6a**). Protein blot analysis of cells expressing the Kozak-polyleucine-ORF construct (k-Exon-A) shows that the tagged-polyleucine protein migrates as a smear at the top of the gel (**Fig. 6b**). However, we did not detect any tagged-polyleucine protein in cells expressing the Exon-A construct (lacking the Kozak sequence) or the Kozak-stop-polyleucine-ORF construct (k-Stop-Exon-A) (**Fig. 6b**). Although the stop codon in the polyleucine ORF prevented translation of the tagged protein (**Fig. 6b**), we still detected the smaller 1C2-positive protein in cells transfected with all three SCA8 expansion constructs but not in controls (**Fig. 6c**), indicating the 1C2 protein is not translated in the CUG-polyleucine frame.

To define the reading frame encoding the 1C2-positive protein, we performed *in vitro* translation of tagged proteins in each of the three reading frames in the CTG direction (polyalanine, polycysteine and polyleucine) and the CAG reading frame from the opposite direction (**Fig. 6d**). We found that each of the tagged proteins was expressed (**Fig. 6e**), but only the tagged polyglutamine expansion protein was also positive for the 1C2-antibody (**Fig. 6f**), producing a soluble protein of ~40-kDa. These data demonstrate that the 1C2-positive

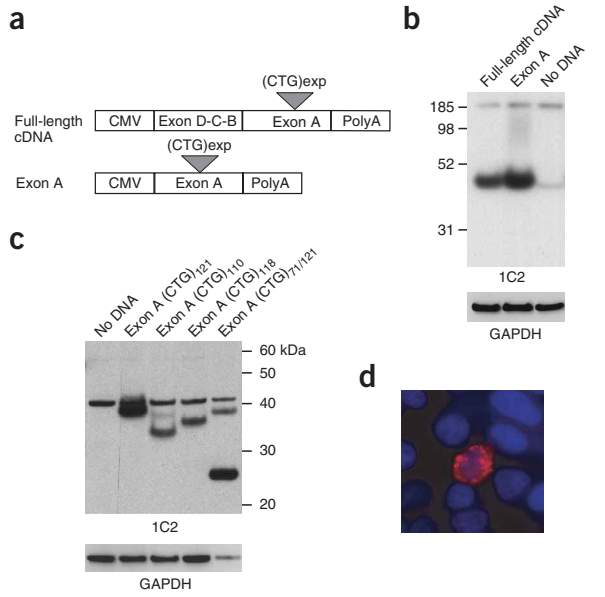

Figure 5 Full-length and truncated (exon A only) *ATXN8OS* cDNAs are capable of producing 1C2 protein, with size dependant upon repeat length. (**a**) Plasmid constructs used for transfection into HEK293 cells. (**b**) Protein blot of lysates from transfections of constructs shown in **a** with immunodetection using antibody 1C2. (**c**) Transfections done with constructs containing varying repeat lengths lead to size variation in the 1C2 proteins detected after transfection. The additional constant 41-kDa protein recognized by the 1C2 antibody in both transfected and untransfected control cells results from the reaction of the 1C2 antibody to endogenous human TATA-binding protein, which contains approximately 40 polyglutamines[50]. Membranes used in **b** and **c** were reprobed with antibody to GAPDH as a loading control (below). (**d**) The protein found in HEK293 cells transfected with the exon A expansion construct form 1C2-positive nuclear and perinuclear aggregates.

protein translated from the SCA8 expansion is not encoded by any of the codons on the CUG strand (that is, $(CUG)_n$-polyleucine, $(UGC)_n$-polycysteine or $(GCU)_n$-polyalanine).

Because these data suggest that the 1C2 protein is generated after transcription and translation from the opposite CAG strand, we examined whether sequence upstream of the SCA8 repeat in the CAG direction is sufficient to drive expression of the 1C2-positive protein using constructs shown in **Figure 7a**. The 1C2 protein was robustly expressed in both orientations (**Fig. 7b**), and expression of the 1C2 protein was still present after removal of both the CMV and SV40 promoters from the pcDNA3.1 vector (**Fig. 7b**), suggesting that endogenous promoter activity upstream of the repeat tract in the CAG direction is responsible for expression of CAG-containing transcripts that are subsequently translated into a 1C2-positive polyglutamine protein. The relative increase in expression of the 1C2-positive band when the repeat is expressed in the CAG or ExonA-Rev orientation versus the CTG orientation is likely to reflect the increased steady-state levels of the CAG transcripts resulting from the inclusion of a strong poly-A signal in the ExonA-Rev and ExonA-Rev (no promoter) constructs.

To confirm that the 1C2-positive protein was translated in the CAG reading frame, we tested tagged constructs for all three frames (**Fig. 7c**). As expected, all three constructs produced a 1C2-positive protein; however, only the construct expressing the tag in the glutamine frame generated a 1C2-positive band that was also positive for the His tag (**Fig. 7d**). These data demonstrate that translation of the SCA8 repeat expansion in the glutamine frame is responsible for the 1C2-positive protein and strongly suggest that the 1C2-positive inclusions found in our BAC-Exp mice and human SCA8 autopsy tissue contain a polyglutamine expansion protein encoded by SCA8 CAG expansion transcripts.

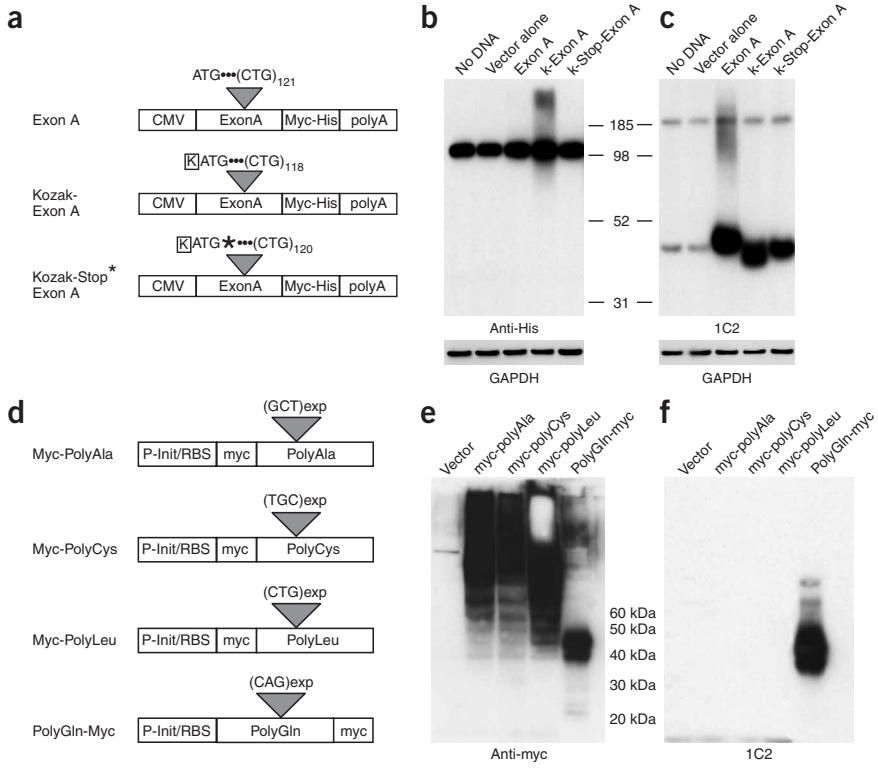

Figure 6 1C2 protein made from the *ATXN8* cDNA results from translation of a polyglutamine ORF. (**a**) Schematic diagrams of constructs used for transfections into HEK293 cells. K: Kozak consensus sequence. *: stop codon. (**b**,**c**) Protein blots of lysates from HEK293 cells after transfections with constructs shown in **a**. Immunodetection was done using either antibody to His (**b**) or the 1C2 antibody (**c**). As in **Figure 5b,c**, the additional constant 41-kDa protein recognized by the 1C2-antibody in untransfected cells and cells transfected with empty vector result from the reaction of the 1C2 antibody to endogenous human TATA-binding protein containing ~40 glutamines. The constant band at higher molecular weight (>100 kDa) appeared in all lanes (**b**,**c**) with comparable intensity including negative controls indicating this band is a nonspecific background band. Membranes used in **b** and **c** were reprobed with antibody to GAPDH as a loading control (below). (**d**) Constructs used for *in vitro* translation experiments tagged in various reading frames. (**e**,**f**) Protein blot of *in vitro* translation products using constructs in **d** with antibody to myc (**e**) or 1C2 antibody (**f**).

Transcripts expressed in CAG direction in mice and humans

In our initial SCA8 report describing strand specific RT-PCR of human cerebellar RNA, we used primers flanking the repeat tract but did not detect transcripts spanning the repeat on the CAG strand[2]. To circumvent potential problems in reverse transcription or amplification across the expansion, we designed a new set of strand specific RT-PCR primers to amplify transcripts 3′ of the repeat in the CAG direction (**Fig. 7e**) and show that the SCA8 locus is transcribed in the CAG direction in BAC-Exp, BAC-Ctl, human control and human SCA8 cerebellar RNA (**Fig. 7f**). The nontransgenic animal served as a negative control, as the SCA8 repeat region is not conserved in mouse. To ensure that RT-PCR products were amplified from the CAG but not the CUG strand, strand specific primers (**Fig. 7e**) containing a 5′ extension ('linker') were used to generate linker-tailed first strand products that can only be subsequently amplified after a primer complimentary to the primed sequence makes a complimentary copy of the specific linker sequence (**Fig. 7f**). CAG containing transcripts in BAC-Exp animals were detectable throughout the

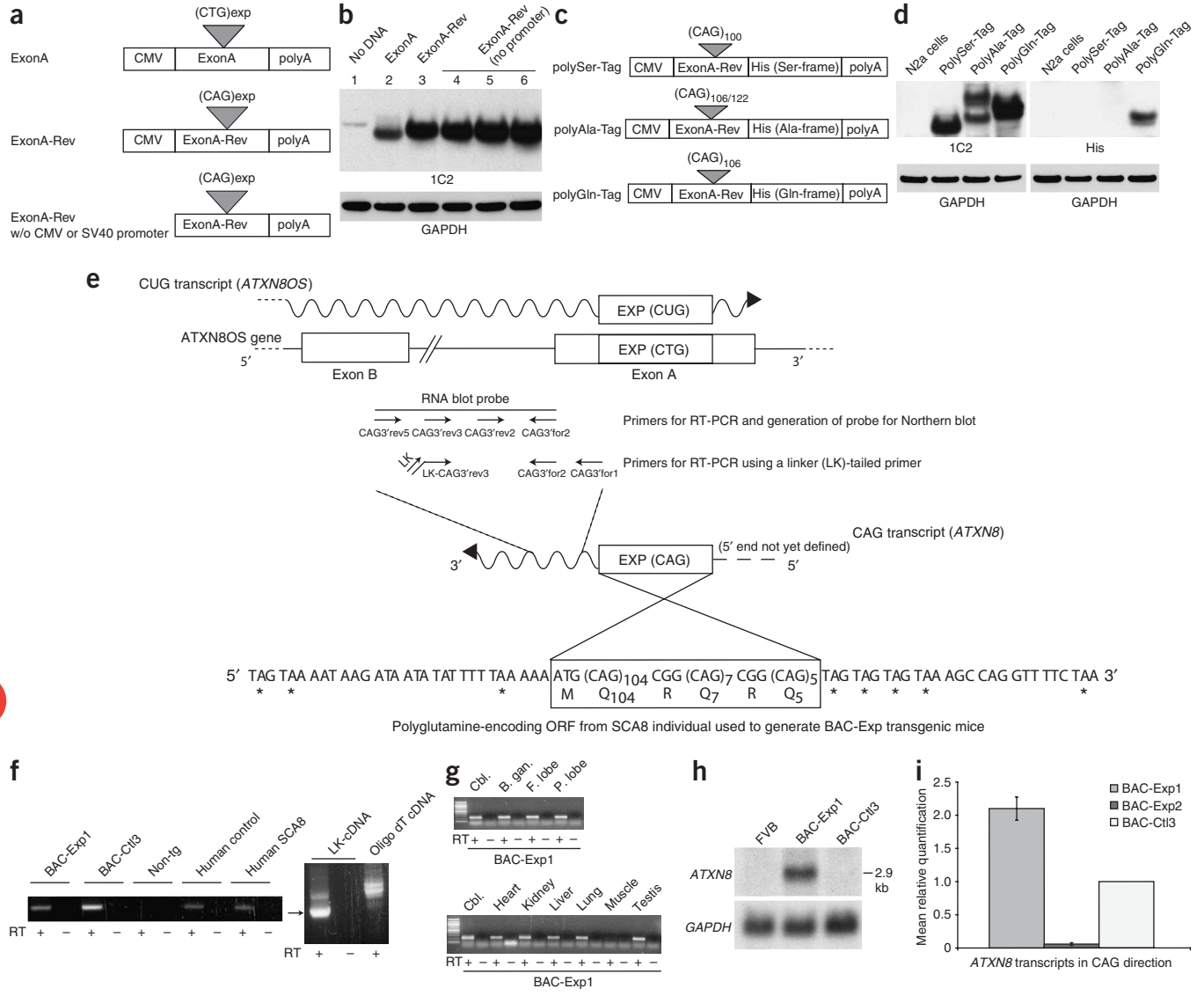

Figure 7 Endogenous promoter activity, translation of polyglutamine protein and detection of CAG-containing *ATXN8* transcripts in BAC transgenic mice and humans. (**a**) Constructs oriented in the CAG or CTG directions used to transfect HEK293 cells with and without promoter region. (**b**) Protein blot of lysates from transfections of constructs shown in **a** using the 1C2 antibody. (**c**) Schematic diagram of constructs used to express the SCA8 expansion in the CAG direction with 3′ His tag in each of three possible frames. (**d**) Protein analysis of HEK293 lysates after transfection with constructs shown in **c**. Immunodetection with 1C2 antibody or antibody to His. Membranes used in **b** and **d** were reprobed with antibody to GAPDH as a loading control. (**e**) Diagram showing 3′-regions of overlapping *ATXN8* and *ATXN8OS* genes and their corresponding transcripts (wavy lines). Relative locations of primers for RT-PCR and probe for RNA blot analysis are shown. LK-CAG3′rev3 and LK refer to linker- and linker-tailed primers. The expanded repeat tract on each strand is boxed, and the polyglutamine-encoding ORF on the CAG *ATXN8* transcript is shown. *: stop codons. (**f**) Expression of *ATXN8* CAG transcripts in cerebella of transgenic mice, humans and nontransgenic FVB animals as negative control. (**g**) RT-PCR of ATXN8 transcripts. cerebellum (Cbl.), basal ganglia (B. gan.), frontal (F) and parietal (P) lobes and other tissues. (**h**) RNA blot of BAC-Exp1, BAC-Ctl3 and FVB (negative control) cerebellar RNA. (**i**) Histogram showing mean relative quantification values of RT-PCR analysis of *ATXN8* CAG transcripts in BAC-Exp1, BAC-Exp2 and BAC-Ctl3 lines. Error bars indicate s.e.m. of the dCt values for each group.

CNS including cerebellum, basal ganglia, frontal lobe, parietal lobe and some non-CNS tissues including heart, kidney, liver, lung and testis, but not in skeletal muscle (**Fig. 7g**) or normal human lymphocytes (data not shown). RACE analysis identified a putative polyA signal and 3′ end ~1.5 Kb 3′ of the CAG repeat, within intron A of the overlapping gene, and ~29.5 Kb upstream of the *KLHL1* promoter (**Figs. 1a** and **7e**). Using a probe to specifically detect CAG transcripts, we detected a 2.9-kb band by RNA blot in the BAC-Exp1 ($n = 4$) animals, which have the highest copy number, but not in BAC-Exp2 ($n = 1$) or BAC-Ctl3 ($n = 4$) animals (**Figs. 7e** and **7h** and data not shown) suggesting 2.9 Kb may be the size of one possible transcript expressed in the CAG direction. However, transfection experiments (**Figs. 6a** and **6b**) suggest promoter activity closer to the repeat tract and experiments to define the 5′ end of the CAG transcript(s) still need to be performed.

Quantitative RT-PCR showed that relative transcript levels in the CAG direction in BAC-Ctl3 animals were comparable to the BAC-Exp1 animals and higher than in BAC-Exp2 animals (RQ = 2.1 for BAC-Exp1 versus BAC-Ctl (ANOVA $F_{2,6} = 59.32$, $P = 0.188$); RQ = 0.06 for BAC-Exp2 versus BAC-Ctl3 ($P = 0.0006$); **Fig. 7i**). Although the higher mean RQ values in the BAC-Exp1 versus BAC-Ctl3 animals were consistent with our ability to detect BAC-Exp1 but not BAC-Ctl3 transcripts by RNA blot, the difference in the RQ values was not statistically significant. CAG and CUG transcript levels are both higher in BAC-Ctl3 control animals than in the severely affected BAC-Exp2 line (**Figs. 1h** and **7i**), providing strong evidence that the phenotypic effects in both the high- and low-copy BAC-Exp lines are caused by the expansion mutation.

We were unable to detect the SCA8 polyglutamine expansion protein ataxin 8 by protein blot analysis of cerebellar tissue from our high-copy BAC-Exp lines or human SCA8 autopsy tissue. This technical difficulty, also seen in other polyglutamine disorders[23], is probably caused by a combination of the relatively low *in vivo* expression of the polyglutamine expansion protein and the background signal of the 1C2 antibody on protein blot using cerebellar tissue extracts. As an additional control, we used monoclonal antibodies against the polyglutamine expansion epitope of recombinant DRPLA protein (MW2 and MW5) and obtained similar results for intranuclear inclusions and pan-nuclear staining in Purkinje cells of BAC-Exp mice and SCA8 autopsy brain (**Supplementary Fig. 2** online).

DISCUSSION

We have developed a BAC-transgenic mouse model of SCA8 in which expression of the human gene containing an expansion mutation from an affected individual causes a progressive neurological phenotype not found in BAC control lines. Unexpectedly, both CUG and CAG expansion transcripts are expressed in transgenic animals and human autopsy tissue. The CAG *ATXN8* transcript contains a short ORF that is translated into a nearly pure polyglutamine protein with 1C2-positive inclusions found in Purkinje cells and other neurons in BAC expansion mice and SCA8 human autopsy tissue. SCA8 is the first disease in which the expression of a single trinucleotide expansion mutation from opposite strands produces two molecules known to be pathogenic in other disorders. The expression of both CUG expansion transcripts and a polyglutamine expansion protein suggests that SCA8 involves both protein and RNA gain-of-function mechanisms.

In vivo imaging showing a loss of molecular layer inhibition demonstrates that the BAC-Exp mice have a cerebellar deficit that is likely to contribute to the movement disorder. Molecular layer interneurons are thought to control the timing of Purkinje cell discharge[24–26], with our SCA8-BAC model providing insight into the importance of the cortical inhibitory circuitry. Decreased fluorescence results from deficits in postsynaptic $GABA_A$ receptor activity[25,27] with either pre- or postsynaptic mechanisms causing reduced inhibition in the BAC-Exp mice, with possible deficits including abnormalities in GABA synthesis, release, uptake or receptor function.

Intranuclear inclusions in cerebellar Purkinje and brainstem neurons in BAC expansion lines and human SCA8 autopsy tissue provide a histopathological link between our mouse model and the human disease. The presence of these inclusions led us to investigate the possibility that a short ORF spanning the SCA8 expansion encodes a protein. *In vitro* and *in vivo* experiments have shown that sequence flanking the SCA8 repeat has endogenous promoter activity that drives expression of CAG-containing transcripts with the subsequent translation of a 1C2-positive polyglutamine expansion protein. Our demonstration that tagged-polyleucine protein is not 1C2 positive differs from a previous report[21], however, because colocalization of the 1C2 signal with the tagged polyleucine protein was not demonstrated in that study, the 1C2 signal that they observed may have similarly resulted from the unexpected expression of a polyglutamine protein in the opposite direction.

The reduced penetrance of SCA8 is one of the most controversial and difficult-to-understand features of the disease. Although all Caucasian SCA8 expansion chromosomes arose from a single founder[12], the repeat tract[28] and neighboring flanking sequences[29] are highly mutable. It should be noted that the expansion used in our mouse model, which was cloned from an affected MN-A family member, contains two CCG-CGG interruptions that introduce arginines into the polyglutamine repeat tract. These interruptions, which vary in number and configuration even within the MN-A family[28], are found in all affected members of the MN-A family and may increase the pathogenicity of the SCA8 mutation.

Inclusions are a common histopathological finding in many neurodegenerative disorders, although significant debate has surrounded whether inclusions themselves are pathogenic[30–32]. We find significant functional changes in the cerebellum of our BAC-Exp mice; however, in contrast to human SCA8, no Purkinje-cell degeneration or other neurodegenerative changes are found. A possible explanation for this difference may be that events leading to neurodegeneration in humans do not have sufficient time to develop during the lifespan of a mouse. Another possibility is that the 1C2 inclusions are protective and that mice, which are more efficient than humans at inclusion formation, more efficiently sequester these pathogenic molecules.

Whereas most pathogenic polyglutamine expansions are encoded as part of larger proteins, the *ATXN8* ORF encodes only a single methionine and a stretch of CAG polyglutamine codons (which may contain one or more interruptions) (**Fig. 7e** and **Supplementary Fig. 3** online). The expression of a pure-polyglutamine expansion protein in *Drosophila melanogaster* has been shown to cause 1C2-positive inclusions and a neurodegenerative phenotype, demonstrating that pure-polyglutamine expansion proteins can be pathogenic[33]. In addition to the expression of a potentially toxic polyglutamine expansion protein, BAC-Exp lines and individuals with SCA8 also express CUG expansion transcripts. A substantial body of evidence now demonstrates that transcripts containing CUG or CCUG expansions can trigger disease through *trans*-dominant gain-of-function effects at the RNA level[34–38].

Although pathogenic mechanisms involving CUG expansion transcripts and/or polyglutamine toxicity are likely to contribute to the phenotype in our BAC-Exp mice, another possibility, *KLHL1* dysregulation, seems not to be involved. At the genomic level, the 5′ end of *ATXN8OS* overlaps the 5′ end of an actin-binding protein gene

Kelch-like 1 (*KLHL1*) a gene transcribed in the opposite direction[4,39] (**Supplementary Fig. 4** online). Although a functional relationship between the two transcripts has not been demonstrated, the *ATXN8OS* CUG transcript has been suggested to regulate *KLHL1* through an antisense mechanism[39,40], with further speculation that pathogenic SCA8 repeat expansions lead to *KLHL1* dysregulation. Although our model was not designed to test this hypothesis, homology between the mouse *Klhl1* gene and the 5′ end of the human *ATXN8OS* transcripts could theoretically affect mouse *Klhl1* expression through a *trans*-antisense interaction. Because RNA blot analysis shows that steady-state levels of mouse *Klhl1* are similar in BAC-Exp animals and controls, effects on *Klhl1* are unlikely to contribute to the phenotype in our mice (**Supplementary Fig. 4**).

Although SCA8 is the first reported disease in which a single repeat expansion is expressed as both a polyglutamine protein and a CUG expansion transcript, this bidirectional expression is likely to have parallels to other triplet expansion disorders. For example, CUG expansion transcripts and more recently antisense transcripts spanning the repeat in the CAG direction have been reported at the myotonic dystrophy type 1 (DM1) locus[41]. Similarly, Huntington disease–like 2 (HDL2), another neurodegenerative disease in which CUG expansion transcripts are expressed, is also characterized by 1C2-positive inclusions, suggesting the possibility that bidirectional transcription of the mutation may also be found in that disease[42].

Our BAC-transgenic model demonstrates the pathogenic effects of the SCA8 expansion and provides a model for further characterizing the molecular aspects of this disorder. The recapitulation of the unexpected bidirectional expression of the SCA8 expansion in mice demonstrates the power of studying human mutations using large-insert BAC clones to approximate their human genetic context. Our data combined with the growing number of reports of antisense transcripts expressed in mammals[43] raises the possibility that bidirectional expression across pathogenic microsatellite expansion shown to occur in SCA8 and DM1 (ref. 41) may be common, and that possible pathogenic effects of mutations transcribed from both strands should be considered. Understanding the genetic complexities of SCA8, including the relative contributions that the polyglutamine expansion protein and CUG expansion transcripts play in disease pathogenesis may provide insight into the reduced penetrance of SCA8 and mechanisms involved in other neurodegenerative diseases.

METHODS

Transgene construction and generation of mice. We constructed a BAC containing an SCA8 repeat expansion with the sequence configuration $[(CTA)_3(CTG)_5CCG(CTG)_7(CCG)(CTG)_{104}]$ from an affected individual using homologous recombination, as previously described[19]. A 1-kb DNA fragment containing the expansion was amplified by PCR from the DNA of an affected individual using primers psvfor and psvrev and was cloned into shuttle vector pSV.1*RecA*. We identified a clone that did not contain any PCR-introduced sequence artifacts. This clone was transformed into *E. coli* cells containing BAC RP11-7o24; cotransformants were identified as being resistant to both tetracycline (shuttle) and chloramphenicol (BAC). Clones selected for both the BAC and the shuttle vector were then grown at 43 °C, the temperature at which the shuttle vector's origin of replication is nonfunctional, thus forcing continued antibiotic selection to occur on a single molecule. These cointegrated clones were identified by DNA blot analysis. A proportion of cointegrate molecules spontaneously resolved through an intramolecular recombination event to form an altered BAC that was found to contain the expanded repeat tract by DNA blot. Sequence analysis confirmed that no mutations were introduced during the recombination process. BAC DNAs with both the normal repeat tract and the expansion were purified using a Qiagen purification kit. Circular BAC DNA was injected into FVB/N zygotes at the University of Minnesota Transgenic Mouse Facility, and founders were identified by DNA blot analysis of tail snip DNA. Animal studies were approved by the Institutional Animal Care and Use Committee at the University of Minnesota, and animal care followed the guidelines established by the Institutional Animal Care and Use Committee at the University of Minnesota. A rare SNP that we previously described in the MN-A family, a G→A transition located 90 bp 3′ of the repeat[12], was also incorporated onto the recombinant expansion BAC. The repeat configuration on the unaltered control BAC is $(CTA)_8(CTG)_{11}$, and this clone contains the more common G form of the 3′ SNP.

Left and right ends of the BAC were screened using the primer pairs CGIfor and CGIrev, and CGIIfor and CGIIrev, respectively, in a PCR mixture containing 10 mM Tris (pH 9.0), 50 mM KCl, 0.1% Triton X-100, 0.01% (wt/vol) gelatin, 200 μM dNTPs and 1 unit AmpliTaq (Perkin Elmer) for 35 cycles at 94 °C for 45 s, 55 °C for 45 s and 72 °C for 75 s. Copy number was estimated by DNA blot and densitometry using human genomic DNA as a standard. Consistent with the integration of at least one complete BAC, all of the BAC-Exp lines and two of the three BAC-Ctl lines were positive for both ends of the human BAC insert by PCR analysis. Although the BAC end upstream of the SCA8 locus was not present in the BAC-Ctl2 line, comparable *ATXN8OS* expression with the other control lines suggest that the *ATXN8OS* gene and regulatory regions are intact in this line. The primer sequences used for generation of the BAC-Exp construct and screening of genomic insert ends are shown in **Supplementary Table 1** online.

Survival curves and rotarod analysis. Survival curves for the two high-copy expansion lines show a decreased life span for the BAC-Exp1 ($n = 24$, log rank statistic $P < 0.0001$) and BAC-Exp2 animals ($n = 31$, $P < 0.0001$) compared with BAC-Ctl3 animals ($n = 39$). Rotarod training was performed using an accelerating rotarod (Ugo Basille) as previously described[23]. Four trials were run per day for 4 d; averages of the four trials on day 4 are presented. ANOVA followed by post-hoc analysis (Student's *t*-test) was performed to assess differences in rotarod performance between the BAC expansion, BAC control and nontransgenic littermates. Statistically significant differences (day 4 ANOVA, post hoc *t*-test) from nontransgenic littermates were found in lines BAC-Exp2 ($P = 3 \times 10^{-4}$), BAC-Exp4 ($P = 4 \times 10^{-4}$) and BAC-Exp1 ($P = 9 \times 10^{-6}$).

Immunohistochemistry. For immunohistochemistry, animals were perfused with 12% (wt/vol) buffered formalin using intracardial puncture. Brains were removed and fixed in this same solution overnight at 25 °C. For calbindin staining, 50 μm sections were cut using a vibratome and were placed in PBS. Sections were microwaved in 0.01 M urea three times for 15 s and then blocked in 2% (vol/vol) goat serum, 0.3% Triton X-100 in PBS overnight at 4 °C. Sections were then incubated with calbindin antibody (Sigma) diluted 1:500 in the same blocking solution for 48 h at 4 °C, washed in PBS four times (20 min each) and incubated with secondary antibody (Alexa 488 goat anti-mouse IgG, Molecular Probes) using a 1:500 dilution for 48 h at 4 °C. Sections were then washed in PBS as described above and mounted in glycerol-gelatin containing 4 mg/ml *n*-propylgalate. Stained sections were analyzed using confocal microscopy (BioRad model MRC 1000 mounted to a Nikon Optiphot microscope).

For immunostaining of glial fibrillary acidic protein (GFAP), polyglutamine (1C2, MW2 and MW5), ubiquitin, TATA-binding protein (TBP) and hematoxylin and eosin staining, brains were embedded in paraffin and 5 μm sections were cut using a microtome. These sections were incubated in 0.3% (vol/vol) H_2O_2 for 30 min to bleach endogenous peroxidase activity. One or two antigen-enhancing pretreatments were used for the immunostaining: (i) heating by steamer in 10 mM citrate buffer at pH 6.0 (for GFAP) and (ii) incubation in concentrated formic acid for 5 min (for 1C2, MW2, MW5, TBP and ubiquitin). Sections were blocked in 5% (vol/vol) normal serum from animals in which secondary antibodies were made. Slides were incubated with antibody in blocking solution overnight at 4 °C. Antibody dilutions were as follow: GFAP (BioGenex), 1:1,000; 1C2 (Chemicon), 1:16,000; MW2 and MW5 (Developmental Studies Hybridoma Bank), 1:1,000; TBP (QED Bioscience), 1:20,000; and ubiquitin (Dakocytomation), 1:1,000. Positive staining was visualized by the avidin-biotin-peroxidase complex method (Vector) with diaminobenzidine as the chromogen and counterstained with hematoxylin.

Detection of transgene expression by RT-PCR. For detection of *ATXN8OS* CUG transcripts from the BAC-Exp and BAC-Ctl lines that contain exon A, 5 μg of total RNA from cerebellum was reverse transcribed using SCA8-specific primer 2 or primer 1 and Superscript II, following the manufacturer's suggested protocol (Invitrogen). Ten percent of this reaction was subjected to PCR with primers 5 and 3 as described above. A second round of PCR with 1 μl of round 1 product was performed with primers internal to the first set (nested primer 5 and nested primer 3) under the same reaction conditions. For detection of transcripts ending in exon B′, 5 μg of total RNA was reverse transcribed using primer 4 or an oligo dT primer under the conditions described above. Ten percent of this reaction was subjected to PCR with primers 5 and 6, followed by a second round of PCR with nested primers 5 and 6.

For *ATXN8* CAG transcripts, reverse transcription was performed using gene-specific primer CAG3′rev3, and 5% of this reaction was PCR amplified using primers CAG3′rev2 and CAG3′for2. For linker-tailed transcripts, reverse transcription was done using 5′ linker-tailed primer LK-CAG3′rev3, and two nested rounds of amplification were performed, the first with LK and CAG3′for1 and the second with LK and CAG3′for2. The 3′ extent of the *ATXN8* transcript was determined using 3′ RACE. First-strand synthesis was performed using GeneRacer oligo dT primer (Invitrogen), followed by two rounds of nested PCR using primer pairs GeneRacer 3′ primer (Invitrogen) with CAG3′for2, and GeneRacer 3′ nested primer (Invitrogen) with CAG3′for3. The primer sequences used for detection of the SCA8 CAG (*ATXN8*) and CUG (*ATXN8OS*) transcripts are shown in **Supplementary Table 1**.

Quantitative RT-PCR was used to measure relative gene expression levels. Two- step RT-PCR was performed on an ABI Prism 7500 Real Time PCR System (Applied Biosystems). Total RNA was isolated from mouse cerebellum and cDNA was generated using First-Strand Synthesis Supermix primed with random hexamers (Invitrogen). We used quantitative RT-PCR SYBR Green Master Mix UDG with ROX reference dye (Invitrogen). For detection of *ATXN8OS* transcripts in the CTG direction, we performed PCR with 5% of cDNA product and primers 7 and 8. For detection of *ATXN8* transcripts in the CAG direction, we performed PCR with 5% of cDNA product and primers CAG3′for2 and CAG3′rev2. Two-stage PCR was performed for 50 cycles (95 °C for 15 s, 60 °C for 1 min) in an optical 96-well plate, with each sample cDNA and primer pair performed in triplicate, for a total of three animals per genotype group. Relative quantification compared with BAC-Ctl3 animals was estimated using the threshold cycle (CT) of the *ATXN8* and *ATXN8OS* transcripts for the CAG and CTG direction normalized to the CT of the housekeeping gene HPRT cDNA. Dissociation curve and ethidium bromide gel analysis was used to assess PCR product purity at the end of each quantitative PCR run. Statistical analysis was done using repeated measures ANOVA on the mean normalized CT values ($n = 3$). Graphs are plotted in relative quantification values normalized to BAC-Ctl3 animals. The primer sequences used for quantitative RT-PCR analysis are shown in **Supplementary Table 1**.

Electromyography and muscle histology. Mice were anesthetized with avertin (0.75 mg/g body weight). Spontaneous muscle electrophysiological responses and motor unit potentials were recorded from quadriceps and gastrocnemius muscles of anesthetized mice using Medtronic/Dantec 25-gauge concentric electromyography needles and a Medtronic/Dantec Counterpoint electromyography device. No abnormal spontaneous activity was seen, and motor unit potentials had normal size, configuration and recruitment, with low firing frequency consistent with the level of anesthesia.

Routine muscle histochemistry and light microscopy was performed on frozen muscle sections using the following stains: hematoxylin and eosin (H&E), PAS stain for glycogen, oil red O stain for lipid, Congo red, Gomori trichrome, ATPase (pH 4.35, 4.5 and 9.4), metachromatic ATPase, NADH, succinyl dehydrogenase, modified SDH, COX, α-glycerol phosphate, acid phosphatase, phosphorylase, myoadenylate deaminase and nonspecific esterase.

Animal preparation and flavoprotein autofluorescence optical imaging. Mice (5–17 months old, 30–40 g) were anesthetized with urethane (2.0 mg/g body weight) and supplemented as needed. The animals were artificially respirated with a respirator designed for small stroke volumes and high ventilation rates with brief inspiration times. Core temperature was maintained with a feedback-controlled heating pad. The animal was placed in a stereotaxic frame, Crus I and II of the cerebellar cortex were exposed and the dura removed. An acrylic chamber was constructed around the exposed folia, and they were superfused with normal Ringer's solution[44,45].

The mouse and stereotaxic frame were placed on a large stage with precision X and Y translation beneath the optics from a modified Nikon epifluorescence microscope. Illumination was provided by a 150-W xenon-mercury lamp powered by a stabilized D.C. power source (Opti-Quip). For flavoprotein imaging, excitation light was passed through a band-pass filter (420–490 nm) and the emitted epifluorescence was passed through a long-pass filter (>515 nm) using a 500-nm dichroic mirror. Images were taken with a high-speed, cooled CCD camera and controller (Quantix 57, Roper Scientific) with a 535 × 512 chip using 12-bit digitization at 3 MHz. Final pixel resolution was ~10 × 10 μm. The camera was focused just below the surface of the cerebellar cortex to within the molecular layer.

To activate parallel fibers and their postsynaptic targets (Purkinje cells and interneurons) an epoxylite-coated tungsten microelectrode (~5 MΩ) was placed just into the molecular layer. In all lines, electrical stimulation of parallel fibers elicit a beam of increased fluorescence visible on the surface of Crus II caused by parallel fiber synaptic excitation of Purkinje cells and interneurons[45,46]. Lateral to the beam (that is, off-beam) in normal mice, parallel fiber stimulation also evokes parasagittal patches of decreased fluorescence, representing molecular layer inhibitory activity[47].

A train of stimuli was used (100-μs pulses at 10 Hz for 10 s), testing the on- and off-beam responses at both 50 and 200 μA. Stimulation at 50 μA was tested, as molecular layer inhibitory interneurons are known to respond at low stimulation strength[48]. The basic imaging paradigm consists of collecting a time series of images before, during and after application of the stimulus. Typically, ten background frames (200-ms exposure) were collected before the application of stimulus, representing the baseline epifluorescence. Next, a series of experimental images was taken during and after stimulation. Metamorph Imaging System (Universal Imaging Corp.) was used to control the camera, shutters and stimulators and to perform basic image processing operations. Having obtained a series of images, we determined the optical response by subtracting the average of the background images from all the images acquired. After subtraction of the background image, the result was a series of 'resultant' images that include ten pre-stimulation 'control' images (background-background) and images consisting of the changes in epifluorescence during and after stimulation. Quantification of the optical signal in each experimental image (F_e) in the series was based on the net fluorescence change (ΔF) in a region of interest as a function of the fluorescence in the background image (F_B): $\Delta F/F = (F_e - F_B)/F_B$. Then the average $\Delta F/F$ in the region of interest was determined. The regions of interest were either the beam of increased fluorescence or the parasagittal patches of decreased fluorescence evoked by parallel fiber stimulation. ANOVA followed by Duncan's post hoc test was used to test for statistical differences between the BAC-Exp2 mice and the control mice (nontransgenic FVB and BAC-Ctl3). To quantify the effect of bicuculline (Bic) on the optical responses, the percentage change relative to the baseline response was determined $(\Delta F/F_{Bic} - \Delta F/F_{Baseline})/\Delta F/F_{Baseline}$. Because an off-beam negative response after bicuculline application could become a net increase in fluorescence, reductions greater than 100% were possible.

The optical responses were displayed by superimposing statistically significant fluorescence changes evoked by parallel fiber stimulation onto an image of the background fluorescence[49]. The threshold for significance was defined as any pixel with a value greater than or less than 2.5 standard deviations of the mean background fluorescence. Increases in fluorescence were pseudocolored using yellow to red and decreases in fluorescence using green to blue.

cDNA constructs. ExonA of *ATXN8OS* containing the expansion was amplified by PCR from the BAC transgene construct, BAC-Exp, using the 5′ primer BAC-Con5′, containing an added *Hin*DIII restriction site, and the BAC-Con3′ primer, containing an added *Xba*I restriction site. This *Hin*DIII/*Xba*I fragment was cloned into the pcDNA3.1/*myc*-His A vector (Invitrogen). The *ATXN8OS* ExonA cDNA was placed under the control of the CMV promoter of plasmid pcDNA3.1/*myc*-His, and the *myc*-His epitope was produced in the polyleucine reading frame. To generate k-ExonA, the bases around the AUG start codon in the 5′ primer were modified to match the Kozak consensus sequence. The

k-stop-ExonA construct was generated by modifying the codon right after the AUG of k-ExonA to a stop codon. A PCR product that contains exons D, C and B of *ATXN8OS* was subcloned into pcDNA3.1-ExonA to generate the full-length cDNA construct containing exons D, C, B and A. To construct ExonA-Rev, the *Hin*DIII/*Xba*I fragment of *ATXN8OS* ExonA was subcloned in the reverse orientation into pcDNA3.1/*myc*-His vector. For ExonA-Rev (without CMV or SV40 promoters), the CMV promoter was removed from ExonA-Rev using *Bgl*II and *Bam*HI digestion followed by blunt-end ligation, and the SV40 promoter was deleted using *Dra*III and *Bst*Z17I digestion and ligation. To generate the poly-Ser-Tag, poly-Ala-Tag, and poly-Gln-Tag constructs (**Fig. 7c**), the CGG interruption at the 3′ end CAG repeats of the *Hin*DIII/*Xba*I fragment as described above was digested with *Msp*A1I to remove the 3′ sequence of ExonA in the CAG direction and several stop codons immediately following the polyglutamine ORF. This fragment was subcloned into pcDNA3.1/*myc*-His in each of three reading frames (A, B and C, respectively). In the three resulting constructs, polyserine, polyalanine and polyglutamine are individually cloned in frame with a *myc*-His tag. The integrity of all constructs was confirmed by sequencing. The primer sequences used for generation of cDNA constructs for cell culture study are shown in **Supplementary Table 1**.

Cell culture and transfection. HEK293 cells lines were cultured in DMEM supplemented with 10% (vol/vol) fetal bovine serum and incubated at 37 °C in a humid atmosphere with 5% CO_2. Transfections were performed using Lipofectamine 2000 Reagent (Invitrogen), according to the manufacturer's instructions.

***In vitro* translation.** An alanine repeat (GCT_{108}), a leucine repeat (CTG_{113}), a cysteine repeat (TGC_{105}) and a glutamine repeat (CAG_{104}) were PCR amplified starting from a cloned CTG-CAG repeat and were tagged with *myc* either 5′ to the start codon (alanine, leucine and cysteine) or 3′ to the repeat (glutamine) in Ambion Pro Vector from the Ambion Pro prokaryotic *in vitro* translation kit. Coupled transcription and translation were performed using 0.5 μg of each plasmid, and 10% of each reaction was immunoblotted as described below.

Immunoblotting. Cells on 60-mm cell culture plates were rinsed with PBS and lysed in 450 μl RIPA buffer (150 mM NaC1, 1% (wt/vol) sodium deoxycholate, 1% Triton X-100, 50 mM Tris-HC1 pH 7.5, 100 μg/ml phenylmethylsulfonyl fluoride (PMSF)) for 45 min on ice. DNA was sheared by passage through a 21-gauge needle. The cell lysate were centrifuged at 16,000*g* for 15 min at 4 °C, and the supernatant was collected. The protein concentrations of cell lysate were determined using the protein assay dye reagent (Bio-Rad). We separated 20 μg of protein on a 10% NuPAGE Bis-Tris gel (Invitrogen) and transferred it to nitrocellulose membrane (Amersham). The membrane was blocked in 5% (wt/vol) dry milk in PBS containing 0.05% (vol/vol) Tween 20 and was probed with the anti-His antibody (1:500) or 1C2-antibody (1:1,000) in blocking solution. After incubating the membrane with HRP-conjugated secondary antibody to rabbit or to mouse (Amersham), bands were visualized by the ECL Plus Protein Blotting Detection System (Amersham).

RNA blot analysis. For RNA blot analysis, 15 μg of total RNA isolated from nontransgenic FVB, BAC-Exp, and BAC-Ctl cerebellum was separated on a NorthernMax-Gly glyoxal gel (Ambion), transferred to a nitrocellulose membrane, cross-linked by ultraviolet radiation and hybridized at 65 °C in Rapid-Hyb buffer (Amersham) using a [^{32}P]dATP-labeled PCR probe. For CAG-containing *ATXN8* transcripts, PCR primers CAG3′for2 and CAG3′rev5 were used to generate the probe. The probe used to detect the mouse *Klhl1* transcripts was generated by PCR using primers kelchfor and kelchrev. This 605-bp probe is specific to exons 2–5 of the mouse *Klhl1* cDNA. The primer sequences used for generation of RNA blot probes are shown in **Supplementary Table 1**.

Clinical evaluation of affected individuals. The pathological findings we report on the SCA8 brain refer to results of an autopsy of a woman in the MN-A family who died at age 74 years from metastatic breast cancer. When evaluated at 68 years, she denied substantial symptoms of ataxia but on examination showed mild pancerebellar ataxia involving eye movements, speech, gait, dexterity and handwriting. Typical of SCA8, she showed no significant weakness, sensory deficits or corticospinal tract involvement. This individual signed an informed consent form approved by the Human Subjects Committee at the University of Minnesota.

Accession codes. GenBank: *Homo sapiens ATXN8* mRNA, partial sequence, DQ641254; *Homo sapiens ATXN8OS* (formerly *SCA8*) repeat region AF126748; *Homo sapiens ATXN8OS* mRNA (formerly *SCA8* mRNA) AF126749; *Homo sapiens* clone RP11-7O24, AC013772.

URLs. The US National Center for Biotechnology Information database is available at http://www.ncbi.nlm.nih.gov/. The University of California, Santa Cruz Genome Bioinformatics website is http://genome.ucsc.edu/. The Mouse Genome Informatics website is http://www.informatics.jax.org/. The HUGO Gene Nomenclature Committee website is http://www.gene.ucl.ac.uk/nomenclature/.

Note: Supplementary information is available on the Nature Genetics website.

ACKNOWLEDGMENTS

We thank SCA8 family members for their participation; M.S. Swanson for critically reviewing our manuscript; H.T. Orr, M.T. Su, H.M. Hsieh-Li, G.W. Lee-Chen for helpful discussions and D. Norton, A. Rose and A. Koeppen for providing control autopsy tissues. Grant support from the National Ataxia Foundation and the US National Institutes of Health (RO1 NS40389) is gratefully acknowledged.

COMPETING INTERESTS STATEMENT

The authors declare that they have no competing financial interests.

Published online at http://www.nature.com/naturegenetics
Reprints and permissions information is available online at http://npg.nature.com/reprintsandpermissions/

1. Zoghbi, H.Y. & Orr, H.T. Glutamine repeats and neurodegeneration. *Annu. Rev. Neurosci.* **23**, 217–247 (2000).
2. Ranum, L.P.W. & Day, J.W. Pathogenic RNA repeats: an expanding role in genetic disease. *Trends Genet.* **20**, 506–512 (2004).
3. Koob, M.D. *et al.* Rapid cloning of expanded trinucleotide repeat sequences from genomic DNA. *Nat. Genet.* **18**, 72–75 (1998).
4. Koob, M.D. *et al.* An untranslated CTG expansion causes a novel form of spinocerebellar ataxia (SCA8). *Nat. Genet.* **21**, 379–384 (1999).
5. Juvonen, V. *et al.* Clinical and genetic findings in Finnish ataxia patients with the spinocerebellar ataxia 8 repeat expansion. *Ann. Neurol.* **48**, 354–361 (2000).
6. Schols, L. *et al.* Do CTG expansions at the SCA8 locus cause ataxia? Genetic background of apparently idiopathic sporadic cerebellar ataxia. *Ann. Neurol.* **54**, 110–115 (2003).
7. Ikeda, Y. *et al.* Asymptomatic CTG expansion at the SCA8 locus is associated with cerebellar atrophy on MRI. *J. Neurol. Sci.* **182**, 76–79 (2000).
8. Silveira, I. *et al.* High germinal instability of the (CTG)n at the SCA8 locus of both expanded and normal alleles. *Am. J. Hum. Genet.* **66**, 830–840 (2000).
9. Brusco, A. *et al.* Analysis of SCA8 and SCA12 loci in 134 Italian ataxic patients negative for SCA1–3, 6 and 7 CAG expansions. *J. Neurol.* **249**, 923–929 (2002).
10. Day, J.W., Schut, L.J., Moseley, M.L., Durand, A.C. & Ranum, L.P.W. Spinocerebellar ataxia type 8: clinical features in a large family. *Neurology* **55**, 649–657 (2000).
11. Ikeda, Y., Shizuka, M., Watanabe, M., Okamoto, K. & Shoji, M. Molecular and clinical analyses of spinocerebellar ataxia type 8 in Japan. *Neurology* **54**, 950–955 (2000).
12. Ikeda, Y. *et al.* Spinocerebellar ataxia type 8: molecular genetic comparisons and haplotype analysis of 37 families with ataxia. *Am. J. Hum. Genet.* **75**, 3–16 (2004).
13. Worth, P.F., Houlden, H., Giunti, P., Davis, M.B. & Wood, N.W. Large, expanded repeats in SCA8 are not confined to patients with cerebellar ataxia. *Nat. Genet.* **24**, 214–215 (2000).
14. Stevanin, G. *et al.* Are (CTG)n expansions at the SCA8 locus rare polymorphisms? *Nat. Genet.* **24**, 213 (2000).
15. Vincent, J.B. *et al.* An unstable trinucleotide-repeat region on chromosome 13 implicated in spinocerebellar ataxia: a common expansion locus. *Am. J. Hum. Genet.* **66**, 819–829 (2000).
16. Sobrido, M.J., Cholfin, J.A., Perlman, S., Pulst, S.M. & Geschwind, D.H. SCA8 repeat expansions in ataxia: a controversial association. *Neurology* **57**, 1310–1312 (2001).
17. Izumi, Y. *et al.* SCA8 repeat expansion: large CTA/CTG repeat alleles are more common in ataxic patients, including those with SCA6. *Am. J. Hum. Genet.* **72**, 704–709 (2003).

18. Sulek, A., Hoffman-Zacharska, D., Zdzienicka, E. & Zaremba, J. SCA8 repeat expansion coexists with SCA1–not only with SCA6. *Am. J. Hum. Genet.* **73**, 972–974 (2003).
19. Yang, X.W., Model, P. & Heintz, N. Homologous recombination based modification in *Escherichia coli* and germline transformation in transgenic mice of a bacterial artificial chromosome. *Nat. Biotechnol.* **15**, 859–865 (1997).
20. Shakkottai, V.G. *et al.* Enhanced neuronal excitability in the absence of neurodegeneration induces cerebellar ataxia. *J. Clin. Invest.* **113**, 582–590 (2004).
21. Dorsman, J.C. *et al.* Strong aggregation and increased toxicity of polyleucine over polyglutamine stretches in mammalian cells. *Hum. Mol. Genet.* **11**, 1487–1496 (2002).
22. Trottier, Y. *et al.* Polyglutamine expansion as a pathological epitope in Huntington's disease and four dominant ataxias. *Nature* **378**, 403–406 (1995).
23. Burright, E.N. *et al.* SCA1 transgenic mice: a model for neurodegeneration caused by an expanded CAG trinucleotide repeat. *Cell* **82**, 937–948 (1995).
24. Mittmann, W., Koch, U. & Hausser, M. Feed-forward inhibition shapes the spike output of cerebellar Purkinje cells. *J. Physiol. (Lond.)* **563**, 369–378 (2005).
25. Hausser, M. & Clark, B.A. Tonic synaptic inhibition modulates neuronal output pattern and spatiotemporal synaptic integration. *Neuron* **19**, 665–678 (1997).
26. Suter, K.J. & Jaeger, D. Reliable control of spike rate and spike timing by rapid input transients in cerebellar stellate cells. *Neuroscience* **124**, 305–317 (2004).
27. Llano, I. & Gerschenfeld, H.M. Inhibitory synaptic currents in stellate cells of rat cerebellar slices. *J. Physiol. (Lond.)* **468**, 177–200 (1993).
28. Moseley, M.L. *et al.* SCA8 CTG repeat: en masse contractions in sperm and intergenerational sequence changes may play a role in reduced penetrance. *Hum. Mol. Genet.* **9**, 2125–2130 (2000).
29. Martins, S. *et al.* Haplotype diversity and somatic instability in normal and expanded SCA8 alleles. *Am. J. Med. Genet. B Neuropsychiatr. Genet.* **139**, 109–114 (2005).
30. Zoghbi, H.Y. & Orr, H.T. Polyglutamine diseases: protein cleavage and aggregation. *Curr. Opin. Neurobiol.* **9**, 566–570 (1999).
31. Orr, H.T. Beyond the Qs in the polyglutamine diseases. *Genes Dev.* **15**, 925–932 (2001).
32. Orr, H.T. The ins and outs of a polyglutamine neurodegenerative disease: spinocerebellar ataxia type 1 (SCA1). *Neurobiol. Dis.* **7**, 129–134 (2000).
33. Marsh, J.L. *et al.* Expanded polyglutamine peptides alone are intrinsically cytotoxic and cause neurodegeneration in *Drosophila*. *Hum. Mol. Genet.* **9**, 13–25 (2000).
34. Philips, A.V., Timchenko, L.T. & Cooper, T.A. Disruption of splicing regulated by a CUG-binding protein in myotonic dystrophy. *Science* **280**, 737–741 (1998).
35. Mankodi, A. *et al.* Myotonic dystrophy in transgenic mice expressing an expanded CUG repeat. *Science* **289**, 1769–1773 (2000).
36. Liquori, C. *et al.* Myotonic dystrophy type 2 caused by a CCTG expansion in intron 1 of ZNF9. *Science* **293**, 864–867 (2001).
37. Kanadia, R.N. *et al.* A muscleblind knockout model for myotonic dystrophy. *Science* **302**, 1978–1980 (2003).
38. Ranum, L.P.W. & Day, J.W. Myotonic dystrophy: RNA pathogenesis comes into focus. *Am. J. Hum. Genet.* **74**, 793–804 (2004).
39. Nemes, J.P., Benzow, K.A., Moseley, M.L., Ranum, L.P.W. & Koob, M.D. The SCA8 transcript is an antisense RNA to a brain-specific transcript encoding a novel actin-binding protein (KLHL1). *Hum. Mol. Genet.* **9**, 1543–1551 (2000).
40. Benzow, K.A. & Koob, M.D. The KLHL1-antisense transcript (KLHL1AS) is evolutionarily conserved. *Mamm. Genome* **13**, 134–141 (2002).
41. Cho, D.H. *et al.* Antisense transcription and heterochromatin at the DM1 CTG repeats are constrained by CTCF. *Mol. Cell* **20**, 483–489 (2005).
42. Margolis, R.L. *et al.* Huntington's Disease-like 2 (HDL2) in North America and Japan. *Ann. Neurol.* **56**, 670–674 (2004).
43. Katayama, S. *et al.* Antisense transcription in the mammalian transcriptome. *Science* **309**, 1564–1566 (2005).
44. Gao, W. *et al.* Optical imaging of long-term depression in the mouse cerebellar cortex *in vivo*. *J. Neurosci.* **23**, 1859–1866 (2003).
45. Dunbar, R.L. *et al.* Imaging parallel fiber and climbing fiber responses and their short-term interactions in the mouse cerebellar cortex *in vivo*. *Neuroscience* **126**, 213–227 (2004).
46. Reinert, K.C., Dunbar, R.L., Gao, W., Chen, G. & Ebner, T.J. Flavoprotein autofluorescence imaging of neuronal activation in the cerebellar cortex *in vivo*. *J. Neurophysiol.* **92**, 199–211 (2004).
47. Ebner, T.J., Chen, G., Gao, W. & Reinert, K. Optical imaging of cerebellar functional architectures: parallel fiber beams, parasagittal bands and spreading acidification. *Prog. Brain Res.* **148**, 125–138 (2005).
48. Carter, A.G. & Regehr, W.G. Quantal events shape cerebellar interneuron firing. *Nat. Neurosci.* **5**, 1309–1318 (2002).
49. Hanson, C.L., Chen, G. & Ebner, T.J. Role of climbing fibers in determining the spatial patterns of activation in the cerebellar cortex to peripheral stimulation: an optical imaging study. *Neuroscience* **96**, 317–331 (2000).
50. Nakamura, K. *et al.* SCA17, a novel autosomal dominant cerebellar ataxia caused by an expanded polyglutamine in TATA-binding protein. *Hum. Mol. Genet.* **10**, 1441–1448 (2001).